Resonant transmission of light through finite arrays of slits

A. I. Fernández-Domínguez,[1] F. J. García-Vidal,[1] and L. Martín-Moreno[2]

[1]*Departamento de Física Teórica de la Materia Condensada, Universidad Autónoma de Madrid, E-28049 Madrid, Spain*
[2]*Departamento de Física de la Materia Condensada-ICMA, Universidad de Zaragoza, E-50009 Zaragoza, Spain*

Finite-size effects associated with the phenomenon of extraordinary optical transmission are theoretically addressed. We analyze the *N* dependence of the transmission resonances appearing in one-dimensional periodic arrays of *N* slits. For the transmission resonances located close to the period of the array, it is found that the evolution is controlled by the width of the slits. This parameter completely governs the electromagnetic coupling between slits that, in turn, is the key actor in the formation of the collective surface electromagnetic mode responsible for the enhanced transmission. On the contrary, the transmission process associated with the excitation of waveguide resonances inside the slits is almost independent of the number of slits perforated on the metallic film.

PACS number(s): 42.79.Ag, 41.20.Jb, 42.25.Bs, 73.20.Mf

I. INTRODUCTION

Since the discovery of the phenomenon of extraordinary optical transmission (EOT) through two-dimensional (2D) periodic arrays of subwavelength holes,[1] many theoretical and experimental works have been devoted to analyze its one-dimensional (1D) version, i.e., a periodic array of sub-wavelength slits drilled on a metallic film.[2–12] Although this structure has strong similarities with an array of holes, the fact that, for *p*-polarized light and irrespective of the ratio between its width and the wavelength, the fundamental eigenmode inside a 1D slit always propagates makes the physics a bit different from its 2D counterpart. It was soon realized[3] that, apart from transmission resonances spectrally located close to the period of the array (similar to the ones found in 2D arrays of holes[13]), Fabry-Pérot-type resonances could also enhance the transmission through the perforated metal. Subsequently, it was found that these waveguide resonances could also appear in a single slit.[14–21]

One of the aspects that, to our knowledge, has not been explored before is how the two distinct transmission resonant processes appearing in 1D periodic arrays of slits depend on the number of slits, in other words, how many slits are necessary to observe the resonant phenomenon. The aim of this paper is to fill this gap by analyzing theoretically how the transmission spectrum evolves as the number of slits perforated in the metallic film is increased from 1 to infinity. To this end, we apply a general theoretical framework that is able to deal with the scattering properties of an arbitrary collection of indentations disposed on a metallic film.[22,23] Throughout this paper and in order to concentrate the discussion on the finite-size effects, we are going to consider that the metal is a perfect electrical conductor (PEC). Therefore, our results will have quantitative value for perforated metals in the microwave or THz ranges of the electromagnetic (EM) spectrum. On the other hand, it has been demonstrated in some previous works[24,25] that the PEC approximation is an excellent starting point to study 1D perforated metals in the optical regime.

The paper is organized as follows: In Sec. II, we give a brief overview of the theoretical framework. Section III is dedicated to the analysis of the two limiting cases: a single slit and an infinite array of slits. Our results on finite arrays are described in Sec. IV, whereas the general conclusions are raised in Sec. V.

II. THEORETICAL FRAMEWORK

In Fig. 1, we show a schematic view of the most general structure under study, a perfect conducting film of thickness *h* perforated with an array of slits of different widths a_α disposed in any arrangement. The structure is illuminated from the top ($z<0$) by an incident plane wave. Since this system presents translational symmetry along the direction parallel to the slits, we can restrict our analysis to the perpendicular plane where both light polarizations (*s* and *p*) are decoupled. In the calculations presented in this paper, we consider a freestanding film with no dielectric medium inside the slits, i.e., $\epsilon=1$ everywhere except inside the metal. We study the interaction of *p*-polarized light (magnetic field parallel to the slits) with the perforated metallic film as EOT does not appear for *s*-polarized light (electric field parallel to the slits) for freestanding films.[26]

Our formalism is based on a modal expansion of the EM fields in each region of the structure.[27,28] It is able to describe finite arrays of slits as well as infinitely periodic arrays just by assuming that the supercell of length *L* containing the
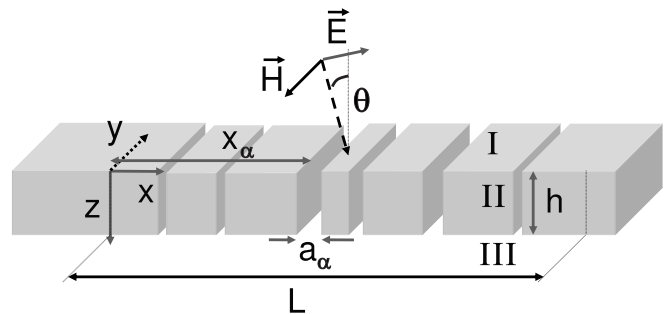
FIG. 1. Schematic view of the most general structure analyzed in this paper: A slit arrangement perforated in a perfect conducting film illuminated by a *p*-polarized plane wave (see text).

array is real (for the infinite case) or artificial (for the finite case), where the limit $L \rightarrow \infty$ must be taken at the end of the numerical procedure. This fact allows us to study the evolution of the transmission properties of finite periodic arrays of slits as the number of slits is increased, and compare them with the well-known infinite case.

The perforated metallic film is illuminated by an incident p-polarized plane wave with wave vector $\vec{k}_0$ ($k_0 = \omega/c = 2\pi/\lambda$) impinging from the top of the film with an angle of incidence θ. The EM fields in region I (see Fig. 1) can be described as the incident plane wave plus a sum of reflected waves weighted with their corresponding reflection coefficients ρ_n. As for the matching procedure, only the parallel components of the EM fields are relevant; it is enough to work with the x component of the electric field and the y component of the magnetic field for p-polarized light. Using Dirac notation,

$$|E_x^{\mathrm{I}}(z)\rangle = |k_0\rangle e^{ik_z^{(0)}z} + \sum_{n=-\infty}^{\infty} \rho_n |k_n\rangle e^{-ik_z^{(n)}z}, \qquad (1)$$

$$|H_y^{\mathrm{I}}(z)\rangle = Y_{k_0}|k_0\rangle e^{ik_z^{(0)}z} - \sum_{n=-\infty}^{\infty} \rho_n Y_{k_n}|k_n\rangle e^{-ik_z^{(n)}z},$$

where $k_n = k_0 \sin\theta + n\frac{2\pi}{L}$ and $k_z^{(n)} = \sqrt{k_0^2 - k_n^2}$. $Y_{k_n} = k_0/k_z^{(n)}$ is the admittance of the p-polarized plane wave $|k_n\rangle$. The plane waves corresponding to the vacuum eigenmodes can be expressed in real space as $\langle x|k_n\rangle = \frac{e^{ik_n x}}{\sqrt{L}}$.

The use of perfect conducting boundary conditions dictates that in region II the EM fields are nonzero only inside the slits. Thus, they can be expanded in terms of slit waveguide modes labeled with two indices referring to the mode order (latin index) and to the slit position inside the array (greek index),

$$|E_x^{\mathrm{II}}(z)\rangle = \sum_{\alpha,m} (A_\alpha^m e^{ig_z^{(\alpha,m)}z} + B_\alpha^m e^{-ig_z^{(\alpha,m)}z})|\alpha,m\rangle,$$

$$|H_y^{\mathrm{II}}(z)\rangle = \sum_{\alpha,m} (A_\alpha^m e^{ig_z^{(\alpha,m)}z} - B_\alpha^m e^{-ig_z^{(\alpha,m)}z}) Y_\alpha^m |\alpha,m\rangle. \qquad (2)$$

The slit waveguide modes in real space are $\langle x|\alpha,m\rangle = \sqrt{\frac{C_m}{a_\alpha}} \cos\left[g_{\alpha,m}\left(x - x_\alpha + \frac{a_\alpha}{2}\right)\right]\theta\left(\frac{a_\alpha}{2} - |x - x_\alpha|\right)$, where $\theta(x)$ is the Heaviside function, $g_{\alpha,m} = m\pi/a_\alpha$, and the normalization constant $C_m = 1$ if $m = 0$ and $C_m = 2$ otherwise. The term $g_z^{(\alpha,m)} = \sqrt{k_0^2 - g_{\alpha,m}^2}$ is the z component of the wave vector corresponding to the mth waveguide mode of slit α, and $Y_\alpha^m = k_0/g_z^{(\alpha,m)}$, its admittance.

In region III (transmission region), EM fields can be written again as a sum over diffraction orders,

$$|E_x^{\mathrm{III}}(z)\rangle = \sum_{n=-\infty}^{\infty} t_n |k_n\rangle e^{ik_z^{(n)}z},$$

$$|H_y^{\mathrm{III}}(z)\rangle = \sum_{n=-\infty}^{\infty} t_n Y_{k_n}|k_n\rangle e^{ik_z^{(n)}z}, \qquad (3)$$

where t_n are the transmission coefficients.

The different expansion coefficients (t_n, ρ_n, A_α^m, and B_α^m) are calculated by imposing continuity of the parallel components of the EM fields at the two interfaces of the system ($z = 0$ and $z = h$). The x component of the electric field must be continuous everywhere at the plane of the interfaces, while the magnetic field must be continuous only at the slit openings. By projecting the x-dependent electric continuity equations (one for each side of the film) over vacuum eigenmodes $\langle k_s|$ and the equations linked to the magnetic field continuity over slit waveguide modes $\langle \beta, l|$, we end up with a system of linear equations of size $2N_{slits}M_{modes}$, where N_{slits} is the number of slits inside the supercell and M_{modes} the number of modes considered inside each slit.

It is appropriate to define the quantities $E_\alpha^m = A_\alpha^m + B_\alpha^m$ and $E'_\alpha^m = -(A_\alpha^m e^{ig_z^{(m)}h} + B_\alpha^m e^{-ig_z^{(m)}h})$, which are related to the m-modal amplitudes associated with the x component of the electric field at both sides of slit α. The system of linear equations that govern E_α^m and E'_α^m behaviors can be written as

$$(G_{\alpha\alpha}^{mm} - \epsilon_\alpha^m)E_\alpha^m + \sum_{l \neq m, \beta \neq \alpha} G_{\alpha\beta}^{ml}E_\beta^l - G_\alpha^{Vm}E'_\alpha^m = I_\alpha^m,$$

$$(G_{\alpha\alpha}^{mm} - \epsilon_\alpha^m)E'_\alpha^m + \sum_{l \neq m, \beta \neq \alpha} G_{\alpha\beta}^{ml}E'_\beta^l - G_\alpha^{Vm}E_\alpha^m = 0. \qquad (4)$$

The different terms appearing in this set of linear equations have a quite simple interpretation. $I_\alpha^m \equiv 2iY_{k_0}\langle \alpha, m|k_0\rangle$ describes the direct initial illumination over the mth waveguide mode of slit α. $\epsilon_\alpha^m \equiv Y_\alpha^m \cot(g_z^{(\alpha,m)}h)$ takes into account the bouncing back and forth of the EM fields associated with mode m inside the same slit α, and $G_\alpha^{Vm} \equiv Y_\alpha^m/\sin(g_z^{(\alpha,m)}h)$ reflects the coupling between the two sides of the slit via mode m.

The term $G_{\alpha\beta}^{ml}$ takes into account that the lth mode in slit β reemits radiation, which is collected by the mth mode in slit α. It controls the coupling between the EM fields inside different slits. This is the only term within the matching equations [Eq. (4)], which changes if we consider an artificial instead of a real supercell. For the case of an infinitely periodic array, it can be written as

$$G_{\alpha\beta}^{ml} \equiv i\sum_{n=-\infty}^{\infty} Y_{k_n}\langle \alpha, m|k_n\rangle\langle k_n|\beta, l\rangle. \qquad (5)$$

By writing $G_{\alpha\beta}^{ml} = \langle \alpha, m|\hat{G}|\beta, l\rangle$, we can define the operator $\hat{G} \equiv i\sum_{n=-\infty}^{\infty} Y_{k_n}|k_n\rangle\langle k_n|$, which couples the EM fields corresponding to different slit waveguide modes through all the diffraction modes in vacuum.

For a finite array, discrete diffraction orders cannot be defined and the spectrum of vacuum eigenmodes becomes continuous. Taking the limit $L \to \infty$, the discrete sum in Eq. (5) transforms into an integral, resulting in a formal expression for the operator $\hat{G}$,

$$\hat{G} = \frac{i}{2\pi} \int_{-\infty}^{\infty} dk_x Y(k_x) |k_x\rangle\langle k_x|, \qquad (6)$$

where now the admittance of the plane wave is a function, $Y(k_x) = k_0 / \sqrt{k_0^2 - k_x^2}$, and the vacuum plane waves are expressed in real space as $\langle x | k_x \rangle = e^{ik_x x}$. Writing this operator in the position basis, we can evaluate the integral, obtaining

$$G(x, x') \equiv \langle x | \hat{G} | x' \rangle = \frac{i\pi}{\lambda} H_0^{(1)}(k_0 |x - x'|), \qquad (7)$$

where $H_0^{(1)}$ is the zero-order Hankel function of the first kind. We find that the function that controls the EM coupling between slits turns out to be the Green's function associated with Helmholtz's equation in two dimensions.[29]

Once the quantities E_α^m and E'^m_α in Eq. (4) are known, EM fields in all spaces can be constructed. The EM power transmitted through the structure is then given by the integral of the z component of the time averaged Poynting vector along the x direction in the far field region. However, due to the absence of losses in our model, this power is equal to the EM energy flowing within the slits in the positive z direction, which in our formalism can be written as

$$P_{EM} = \sum_{\alpha,m} Y_\alpha^m (|A_\alpha^m|^2 - |B_\alpha^m|^2), \qquad (8)$$

where A_α^m (B_α^m) is the electric field amplitude corresponding to the mth waveguide mode at slit α traveling in the positive (negative) z direction [see Eq. (2)]. It is straightforward to demonstrate that the expression for the power transmitted through the structure can be rewritten in terms of E_α^m and E'^m_α as $P_{EM} = \sum_{\alpha,m} \mathrm{Im}(G_\alpha^{Vm*} E_\alpha^m E'^m_\alpha)$.

In what follows, we introduce a further approximation in our numerical calculations. We have demonstrated in previous works[3,24,25] that, in the subwavelength regime ($\lambda \gg a$), it is a very good approximation to consider that only the first waveguide mode ($m=0$) is excited by the incident plane wave. Note that, irrespective of the ratio between a and λ, this first waveguide mode always propagates.

III. INFINITE ARRAY AND SINGLE SLIT

We motivate the study of the transmission properties of finite arrays of slits by first analyzing two interesting and limiting cases in which the matching equations [Eq. (4)] become very simple: the single slit and the infinitely periodic array of identical slits, both systems illuminated by a normal incident plane wave. In spite of being very different systems, in both cases we find that by considering only the first mode inside the slit(s), the system of linear equations simplifies into just the same two equations:
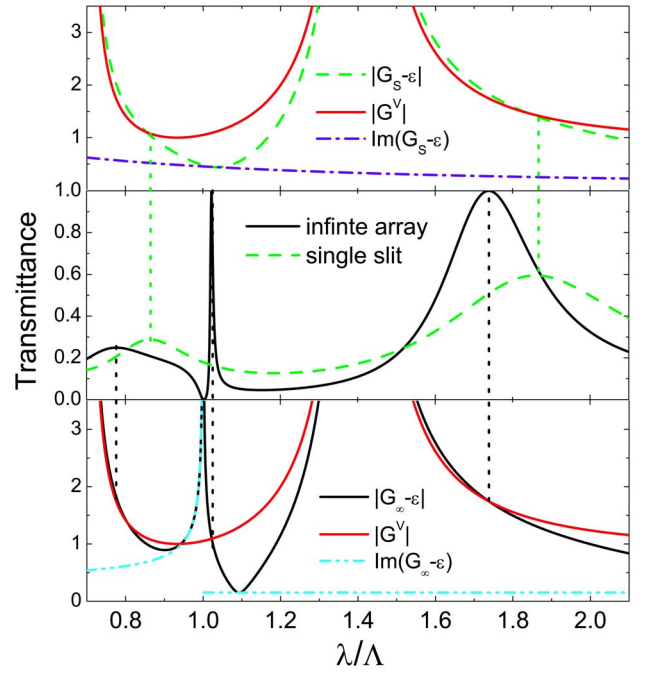
FIG. 2. (Color online) Transmission spectra normalized to the light impinging the area corresponding to the array periodicity (Λ) for a single slit and for an infinite periodic array of slits (for both structures, $h = 0.7\Lambda$ and $a = 0.15\Lambda$). Top: wavelength dependence of the relevant terms in Eq. (9) for the single slit. Bottom: the same but for the infinite array of slits.

$$(G - \epsilon)E - G^V E' = I,$$

$$(G - \epsilon)E' - G^V E = 0, \qquad (9)$$

where for both systems $I = 2i\langle 1 | k_0 \rangle$, $\epsilon = \cot(k_0 h)$, and $G^V = 1/\sin(k_0 h)$ (at normal incidence $k_{n=0} = k_0$). The wave function inside the slits is $\langle x | 1 \rangle = 1/\sqrt{a}$, where a is the slit width and $|1\rangle \equiv |\alpha=1, m=0\rangle$. The only difference between the two systems resides in the expression for G in Eq. (9).

For the single slit case, $G = G_S = \int\int dx dx' \langle 1 | x \rangle G(x, x') \times \langle x' | 1 \rangle$, where the integrals on x and x' run over the width of the slit. On the other hand, for the infinite case, periodic boundary conditions are imposed to the general equations [Eq. (4)]. Since light impinges normally to the array plane ($k_x = 0$), Bloch's theorem states that the value of the EM fields inside all the slits must be the same, i.e., $E_\alpha = E$ and $E'_\alpha = E'$ for all α. The general infinite system of matching equations becomes degenerate, and the only two equations that remain linearly independent can be written in the form of Eq. (9) with $G = G_\infty$,

$$G_\infty = i \sum_{n=-\infty}^{\infty} Y_{k_n} \langle 1 | k_n \rangle \langle k_n | 1 \rangle. \qquad (10)$$

The central panel of Fig. 2 shows the comparison between the transmission spectra for a single slit and for an infinite array of slits. In both cases, the transmittance (defined as the ratio between the EM power exiting and impinging on the structure) is normalized to the EM flux incident on the area

corresponding to the array periodicity (Λ). For the normalization considered, the transmissivity of both structures has the form

$$T = (G^V/Y_{k_0})\mathrm{Im}(EE'^*). \qquad (11)$$

Since we are considering perfect conducting boundary conditions, all lengths in the structure are scalable, and we can take Λ as the unit length. For the two structures analyzed in Fig. 2, the thickness of the film is chosen to be $h=0.7\Lambda$ and the slit width to be $a=0.15\Lambda$. In the wavelength range analyzed, the single slit spectrum presents two maxima, which corresponds to the first two waveguide resonances. As previously reported, they are located near the Fabry-Pérot condition $\sin(k_0 h)=0$. The infinite array spectrum shows these two maxima, too, but shifted to shorter wavelengths. However, slightly above the periodicity ($\lambda \gtrsim \Lambda$), this spectrum presents a strongly peaked feature that does not appear for the single slit. This maximum is associated with the excitation of a surface EM mode, which decorates both sides of the perfect conducting film.[3,7] It is accompanied by a sharp drop in the transmittance just at the periodicity, the well-known Wood's anomaly.

All this phenomenology for a single slit and for an infinite array of slits has been previously discussed.[3] However, our approach allows us to understand the physics and mathematics behind the resonant features by just analyzing the terms appearing in Eq. (9). The wavelength dependence of the different terms in Eq. (9) for a single slit and for an infinite array is shown in the top and bottom panels of Fig. 2, respectively. For example, the origin of Wood's anomaly, present only in the infinite array spectrum, stems from a divergence in G_∞ [see the lower panel in Fig. 2 and Eq. (10)] that appears just at the wavelength in which a diffraction order $(\pm 1,0)$ becomes evanescent ($\lambda=\Lambda$, $k_z=0$), the well-known Rayleigh condition. This divergence makes the field intensity at both the input and exit sides of the slits vanish, i.e., $|E|=|E'|=0$. As in typical resonant phenomena, the spectral locations of the EM modes can be extracted by looking at zeros in the determinant of the matrix defining the associated set of linear equations.[3,30,31] For both structures, the spectral locations of the transmission peaks coincide with cuts between $|G^V|$ and $|G-\epsilon|$. Imposing $|G^V|=|G-\epsilon|$ in Eq. (9), we find that, for wavelengths satisfying this condition, the electric field intensities at both sides of the slits are equal, i.e., $|E|=|E'|$. It is straightforward to demonstrate that this condition also leads to a resonant denominator in the expressions for the corresponding electric field amplitudes $\{E,E'\}$. Therefore, transmission maxima in both spectra rely on EM resonances with the same mathematics but with a very different physical origin.

For a single slit, these resonances are due to the excitation of waveguide resonances with the E field mainly concentrated inside the slits.[14] For an infinite array of slits, these waveguide resonances still emerge in the transmission spectrum, but their locations appear at shorter wavelengths. This shift is due to the EM coupling between the slits forming the infinite array. This EM interaction modifies in an effective way the reflectivity at the boundaries of the Fabry-Pérot cav-
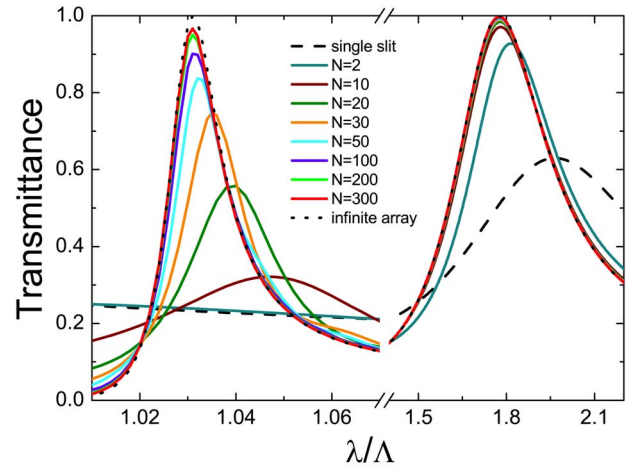
FIG. 3. (Color online) Evolution of the first waveguide resonance and surface EM mode peaks in the transmission spectra for finite arrays of slits as the number of slits is increased. The transmittance is normalized to the EM flux impinging on N times the array periodicity Λ. For all the structures, $h=0.7\Lambda$ and $a=0.2\Lambda$.

ity, changing the spectral location of the corresponding resonance. Additionally, transmission resonances appear close to the divergence of G_∞. It has been shown that this resonance can be seen as a surface EM mode, a *spoof surface plasmon*,[32,33] which originates when the surface of a perfect conductor is periodically corrugated. As a consequence, the E field is maximum at the two interfaces of the metallic film.

IV. FINITE ARRAY OF SLITS

Now, we apply the general formalism described in the first section to the study of the transmission properties of finite periodic arrays of N identical slits. By solving the $2N \times 2N$ system of matching equations [Eq. (4)], we obtain the set of unknowns $\{E_\alpha, E'_\alpha\}$, with α ranging from 1 to N (note that, as in the previous section, we are only taking into account in the modal expansion the first eigenmode inside the slits). Thus, we can calculate the transmittance of the film and evaluate the EM fields at any point of the structure. The expression for the transmittance for a perfect conducting film perforated with a finite array of N slits normalized to the light impinging on the region corresponding to N times the array periodicity ($N\Lambda$) has the form

$$T(N) = \frac{1}{N}\sum_{\alpha=1}^{N} t_\alpha = \frac{G^V}{NY_{k_0}}\sum_{\alpha=1}^{N} \mathrm{Im}(E'_\alpha E_\alpha^*), \qquad (12)$$

where $t_\alpha = (G^V/Y_{k_0})\mathrm{Im}(E'_\alpha E_\alpha^*)$ gives the transmission per slit forming the array (normalized to the array periodicity), i.e., the contribution of each slit to the total transmissivity of the structure. Note that this transmittance is a far field magnitude.

In Fig. 3, we show the transmission spectra of arrays with increasing number of slits. The geometrical parameters of all the structures are $h=0.7\Lambda$ and $a=0.2\Lambda$. We have focused our analysis on the evolution of the peaks at the surface EM mode and the first waveguide resonance.
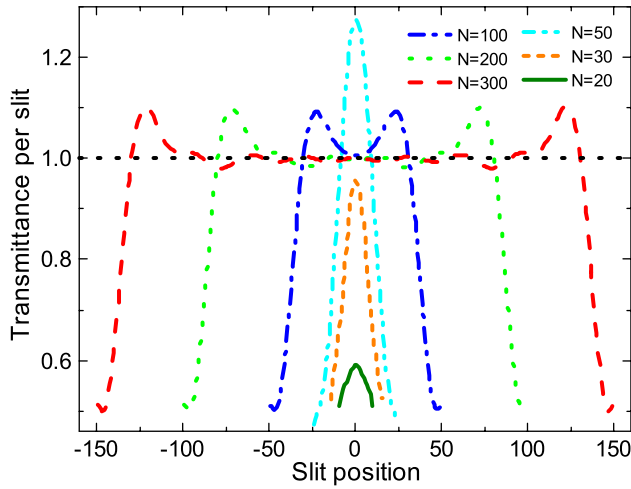
FIG. 4. (Color online) Normalized to periodicity transmission per slit evaluated at the surface EM resonance for arrays of different sizes with $h=0.7\Lambda$ and $a=0.2\Lambda$, as in Fig. 3. The dotted black line corresponds to the uniform transmission pattern for an infinite array of slits.

FIG. 5. (Color online) Transmittance at surface EM resonance calculated from Eq. (12) for different slit widths: $a=0.24\Lambda$ (cyan circles), $a=0.20\Lambda$ (orange up triangles), $a=0.15\Lambda$ (blue squares), $a=0.10\Lambda$ (green down triangles), and $a=0.08\Lambda$ (red rhombuses). For all structures, $h=0.7\Lambda$ Solid lines: fitting curves given by Eq. (13) for $N>N_E$. Inset: linear relation between $2N_E$ and $\lambda_\infty^2/\Delta\lambda_\infty$ for structures with $0.08\lambda \leq a \leq 0.24\Lambda$ and $0.6\Lambda \leq h \leq 0.8\Lambda$.

The first waveguide resonance peak ($\lambda_{res} \simeq 1.75\Lambda$), which already appears in the single slit spectrum, is almost completely formed for an array containing only two slits. This fast development relies on the localized nature of the EM mode involved in the transmission process. Since the coupling and propagation of the incident light through the surface EM mode depend strongly on the corrugation of the structure, light coming from several slits is involved during the corresponding transmission process. It can be seen in Fig. 3 that the surface EM resonance peak ($\lambda_{res} \simeq 1.03\Lambda$) evolves, not only in height but also in linewidth, gradually as the size of the array increases. This fact reinforces the picture of the resonance as a surface EM mode emerging from the collective interaction between slits.

In order to study the effect on the transmittance of the interaction among EM fields coming from different slits, we have plotted in Fig. 4 the normalized to periodicity transmission per slit (t_α) for finite arrays of slits evaluated at the wavelength associated with the surface EM resonance. We have taken the same geometrical parameters as in Fig. 3 ($h=0.7\Lambda$, $a=0.2\Lambda$). For small arrays ($N \leq 100$), the transmittance is maximum at the center of the array. However, for large enough arrays, we can distinguish between two kinds of slit contributions to the total transmittance of the structure. The transmission per slit pattern is composed by a flat central region, whose width grows as the array size is increased, and two edge regions, each of them involving N_E slits, N_E being almost independent of the array size, N. The transmittance through the central ($N-2N_E$) slits is, except some small oscillations, uniform and equal to the value for the infinite case ($T_\infty=1$ for the normalization considered). However, for the N_E slits close to each array edge, t_α falls from 1 to 0.5 as we approach the array ends. It can be seen in Fig. 4 that for the structure considered in our calculation, $N_E \simeq 20$.

Taking advantage of this scalable t_α pattern, we can obtain an approximated expression for the surface EM resonance

peak height as a function of the number of slits for large enough arrays. The transmittance through an array containing N slits can be written as the sum of contributions corresponding to the different regions found in Fig. 4. For the ($N-2N_E$) central slits, the total transmittance is $(N-2N_E)T_\infty = N-2N_E$. For the $2N_E$ edge slits, it results in a good approximation to take the average value of $2N_E[(1+0.5)/2]T_\infty = 3N_E/2$. The transmittance of the array normalized to the EM flux incident on the area corresponding to N times the array periodicity at the surface EM resonance is then given by

$$T_{max}(N) = \frac{1}{N}\left(N - 2N_E + \frac{3N_E}{2}\right) = 1 - \frac{N_E}{2N}. \qquad (13)$$

In Fig. 5, we plot the evolution with N of the surface EM resonance peak height for arrays of slits of different widths (a) perforated in a perfect conducting film of thickness $h=0.7\Lambda$. Dots correspond to values obtained from an exact calculation using Eq. (12). For all the structures, peak growth has a similar behavior. For small arrays, the transmittance depends linearly on N, but for larger ones, it grows much more slowly, going as the inverse of the number of slits, as predicted by Eq. (13). This change in tendency does not occur abruptly at a fixed array size, but in a range whose position and width depend strongly on the width of the slits. The narrower the slits are, the wider this range is. We can relate this two tendencies to the t_α distribution depicted in Fig. 4. For small arrays ($N<2N_E$), the peak height grows linearly, while t_α is peaked around the array center. However, for arrays with $N>2N_E$, the peak goes as the inverse of the slit number, and a flat plateau appears in the transmission per slit pattern. This picture is reinforced by comparing the case analyzed in Fig. 4 ($a=0.20\Lambda$), where the flat plateau is formed for $50<N<100$. The change in tendency for orange up tri-

angles in Fig. 5, which corresponds to the same structure, occurs for $N \sim 70$. Solid lines in Fig. 5 correspond to curves of the form of Eq. (13) fitted to exact calculated values for arrays with $N > 2N_E$. N_E values obtained from the fitting parameters are in very good agreement with the corresponding transmission per slit patterns at resonance. For instance, from Fig. 4, we have $N_E \simeq 20$ for $a = 0.20\Lambda$, and from the fitting curve, we obtain $N_E = 16$.

In the following, we are going to demonstrate that the *phenomenological* parameter $2N_E$ is closely related to the spatial extension of the surface EM mode responsible for the enhanced transmission. This spatial extension can be extracted from the corresponding transmission spectrum for the infinite array. The linewidth of the resonant peak is related to the time ($\Delta\tau$) that EM fields spend during the resonant process before being reemitted from the structure. If we assume that the EM fields associated with the resonant mode travel at the speed of light, the spatial extension of the mode would be $c\Delta\tau = (\lambda_\infty^2/\Delta\lambda_\infty)$, with λ_∞ being the peak position and $\Delta\lambda_\infty$ the linewidth at half maximum of the peak. In the inset of Fig. 5, we represent $2N_E$ versus $(\lambda_\infty^2/\Delta\lambda_\infty)$ (in units of Λ) for the four cases analyzed in the main panel and for others in which the thickness of the metallic film is also varied. This figure clearly demonstrates that there is a linear relation between the two magnitudes, with a proportionality factor being close to 0.4. Although the linewidth of the resonant peak appearing close to the period of the array is a complex function of the geometrical parameters of the structure (a, Λ, and h) and the resonant wavelength, Fig. 5 demonstrates that the main controlling factor is the ratio between the width of the slits and the period of the array.

All the results shown in this paper have been obtained assuming that the perforated metal behaves as a perfect conductor. As said before, our results have semiquantitative values for metals at microwave or THz frequencies. At optical frequencies, it is expected that absorption in the metal would play an important role in the evolution of the transmission spectra as a function of the number of slits. Absorption introduces another lifetime into the problem, the time taken by the photon to get absorbed. Associated with this lifetime, we can introduce a new length scale, L_{abs}, roughly defined as the product of the photon lifetime and the light velocity. If L_{abs} is smaller than $N_E\Lambda$, the number of slits needed to obtain the transmittance of the infinite array will be mainly controlled by absorption in the metal. In the opposite case, transmission resonances can be built up before the photons are absorbed, and hence the values of N_E calculated within the perfect conductor approach still hold.

V. CONCLUSIONS

In conclusion, we have presented a theoretical formalism that is able to analyze finite-size effects appearing in the phenomenon of extraordinary optical transmission through subwavelength slits. We have studied in detail the evolution of the transmission spectra from the single slit case to the limit of an infinite periodic array. We have shown that the number of slits necessary to reach the infinite limit depends strongly on the character of the transmission resonance. For waveguide resonances, two or three slits are enough to observe the saturation both in the location and height of the transmission peak. As a difference, transmission resonances appearing close to the period of the array whose origin stems from the excitation of surface EM modes are extremely sensitive to the number of slits. For this last case, we have demonstrated that there is a close relation between the linewidth of the transmission resonance and the *velocity* in the approach to the infinite limit.

ACKNOWLEDGMENT

[1] T. W. Ebbesen, H. J. Lezec, H. F. Ghaemi, T. Thio, and P. A. Wolff, Nature (London) **391**, 667 (1998).

[2] U. Schröter and D. Heitmann, Phys. Rev. B **58**, 15419 (1998).

[3] J. A. Porto, F. J. García-Vidal, and J. B. Pendry, Phys. Rev. Lett. **83**, 2845 (1999).

[4] M. M. J. Treacy, Appl. Phys. Lett. **75**, 606 (1999).

[5] H. E. Went, A. P. Hibbins, J. R. Sambles, C. R. Lawrence, and A. P. Crick, Appl. Phys. Lett. **77**, 2789 (2001).

[6] Q. Cao and Ph. Lalanne, Phys. Rev. Lett. **88**, 057403 (2002).

[7] F. J. García-Vidal and L. Martín-Moreno, Phys. Rev. B **66**, 155412 (2002).

[8] S. Collin, F. Pardo, R. Teissier, and J. L. Pelouard, Phys. Rev. B **63**, 033107 (2001).

[9] W. C. Liu and Ding Ping Tsai, Phys. Rev. B **65**, 155423 (2002).

[10] Y. Xie, A. Zakharian, J. Moloney, and M. Mansuripur, Opt. Express **12**, 6106 (2004).

[11] K. G. Lee and Q. Han Park, Phys. Rev. Lett. **95**, 103902 (2005).

[12] D. C. Skigin and R. A. Depine, Phys. Rev. Lett. **95**, 217402 (2005).

[13] L. Martín-Moreno, F. J. García-Vidal, H. J. Lezec, K. M. Pellerin, T. Thio, J. B. Pendry, and T. W. Ebbesen, Phys. Rev. Lett. **86**, 1114 (2001).

[14] Y. Takakura, Phys. Rev. Lett. **86**, 5601 (2001).

[15] F. Yang and J. R. Sambles, Phys. Rev. Lett. **89**, 063901 (2002).

[16] H. F. Schouten, T. D. Visser, D. Lenstra, and H. Blok, Phys. Rev. E **67**, 036608 (2003).

[17] J. Bravo-Abad, L. Martín-Moreno, and F. J. García-Vidal, Phys. Rev. E **69**, 026601 (2004).

[18] P. Lalanne, J. P. Hugonin, and J. C. Rodier, Phys. Rev. Lett. **95**, 263902 (2005).

[19] R. Gordon, Phys. Rev. B **73**, 153405 (2006).

[20] C. Wang, C. Du, and X. Luo, Phys. Rev. B **74**, 245403 (2006).

[21] R. Gordon, Phys. Rev. B **75**, 193401 (2007).

[22] J. Bravo-Abad, F. J. García-Vidal, and L. Martín-Moreno, Phys. Rev. Lett. **93**, 227401 (2004).

[23] J. Bravo-Abad, A. Degiron, F. Przybilla, C. Genet, F. J. García-

Vidal, L. Martín-Moreno, and T. W. Ebbesen, Nat. Phys. **2**, 120 (2006).

[24] L. Martín-Moreno, F. J. García-Vidal, H. J. Lezec, A. Degiron, and T. W. Ebbesen, Phys. Rev. Lett. **90**, 167401 (2003).

[25] F. J. García-Vidal, H. J. Lezec, T. W. Ebbesen, and L. Martín-Moreno, Phys. Rev. Lett. **90**, 213901 (2003).

[26] E. Moreno, L. Martín-Moreno, and F. J. García-Vidal, J. Opt. A, Pure Appl. Opt. **8**, 259 (2006).

[27] C. Chen, IEEE Trans. Microwave Theory Tech. **MTT-18**, 627 (1970).

[28] B. Munk, *Frequency Selective Surfaces: Theory and Design* (Wiley, New York, 2000).

[29] G. B. Arfken and H. J. Weber, *Mathematical Methods for Physicists* (Academic, London, 2001).

[30] A. A. Maradudin, A. V. Shchegrov, and T. A. Leskova, Opt. Commun. **135**, 352 (1997).

[31] R. A. Depine and D. C. Skigin, Phys. Rev. E **61**, 4479 (2000).

[32] J. B. Pendry, L. Martín-Moreno, and F. J. García-Vidal, Science **305**, 847 (2004).

[33] F. J. García-Vidal, L. Martín-Moreno, and J. B. Pendry, J. Opt. A, Pure Appl. Opt. **7**, S97 (2005).